Journal of Biomechanics 46 (2013) 165–169

Contents lists available at SciVerse ScienceDirect

Journal of Biomechanics

journal homepage: www.elsevier.com/locate/jbiomech
www.JBiomech.com

Short communication

Serial analysis of lumen geometry and hemodynamics in human arteriovenous fistula for hemodialysis using magnetic resonance imaging and computational fluid dynamics

Yong He [a,b,1], Christi M. Terry [c,1], Cuong Nguyen [c], Scott A. Berceli [a,b], Yan-Ting E. Shiu [c,d,*], Alfred K. Cheung [c,e,*]

[a] Department of Surgery, University of Florida, Gainesville, FL, USA
[b] Malcom Randall Veterans Affairs Medical Center, Gainesville, FL, USA
[c] Division of Nephrology and Hypertension, University of Utah School of Medicine, Salt Lake City, UT, United States
[d] Department of Bioengineering, University of Utah, Salt Lake City, UT, USA
[e] Medical Care Center, Veterans Affairs Salt Lake City Healthcare System, Salt Lake City, UT, USA

ARTICLE INFO

Article history:
Accepted 3 September 2012

Keywords:
Hemodialysis
Arteriovenous fistula
Wall shear stress
Computational fluid dynamics
Magnetic resonance imaging

ABSTRACT

The arteriovenous fistula (AVF) is the preferred form of vascular access for maintenance hemodialysis, but it often fails to mature to become clinically usable, likely due to aberrant hemodynamic forces. A robust pipeline for serial assessment of hemodynamic parameters and subsequent lumen cross-sectional area changes has been developed and applied to a data set from contrast-free MRI of a dialysis patient's AVF collected over a period of months after AVF creation surgery. Black-blood MRI yielded images of AVF lumen geometry, while cine phase-contrast MRI provided volumetric flow rates at the in-flow and out-flow locations. Lumen geometry and flow rates were used as inputs for computational fluid dynamics (CFD) modeling to provide serial wall shear stress (WSS), WSS gradient, and oscillatory shear index (OSI) profiles. The serial AVF lumen geometries were co-registered at 1 mm intervals using respective lumen centerlines, with the anastomosis as an anatomical landmark. Lumen enlargement was limited at the vein region near the anastomosis and a downstream vein valve, potentially attributed to the physical inhibition of wall expansion at those sites. This work is the first serial and detail study of lumen and hemodynamic changes in human AVF using MRI and CFD. This novel protocol will be used for a multicenter prospective study to identify critical hemodynamic factors that contribute to AVF maturation failure.

1. Introduction

The arteriovenous fistula (AVF) is the preferred vascular access for chronic hemodialysis due to lower rates of infection and stenosis than other access types once the AVFs become matured. AVF maturation is characterized by marked luminal dilatation with increased blood flow in the venous portion following its surgical creation. Unfortunately, up to 60% of AVFs never adequately mature (Dember et al., 2008; Biuckians et al., 2008). Typically the lumen fails to enlarge or is reduced by neointimal hyperplasia.

Hemodynamic wall shear stress (WSS) is likely important to the AVF maturation process. Computational fluid dynamics (CFD) analysis of WSS in AVFs has been performed using data obtained from angiography (Ene-Iordache et al., 2001) or MRI (Niemann et al., 2012). However, there has been no published in-depth serial study in human AVF that is essential for understanding the role of WSS in AVF maturation. A multicenter prospective study is currently underway to identify critical hemodynamic factors contributing to AVF maturation or failure. We report here as a proof of concept, the development and application of a robust MRI-to-CFD pipeline to a human AVF (Fig. 1).

2. Methods

2.1. General procedures

This study was approved by the Institutional Review Board at the University of Utah. Written informed consent was obtained from a patient undergoing thrice weekly maintenance hemodialysis using an upper arm brachiocephalic AVF with end-to-side anastomosis. The patient was a 70-year-old female of approximately 50 kg with a body mass index of 21.5 kg/m^2.

Hemodynamic profiles were obtained from CFD analyses using lumen geometry and blood flow boundary conditions acquired by *contrast-free* MRI (Fig. 1) at 4, 5,

* Corresponding authors: Division of Nephrology and Hypertension, University of Utah School of Medicine, 85 North Medical Drive East, Salt Lake City, Utah 84112, USA. Tel.: +1 801 581 6709; fax: +1 801 581 4343.
E-mail addresses: y.shiu@hsc.utah.edu (Y.-T. Shiu), alfred.cheung@hsc.utah.edu (A.K. Cheung).

[1] These two authors contributed equally to this work.

0021-9290/$ - see front matter © 2012 Elsevier Ltd. All rights reserved.
http://dx.doi.org/10.1016/j.jbiomech.2012.09.005

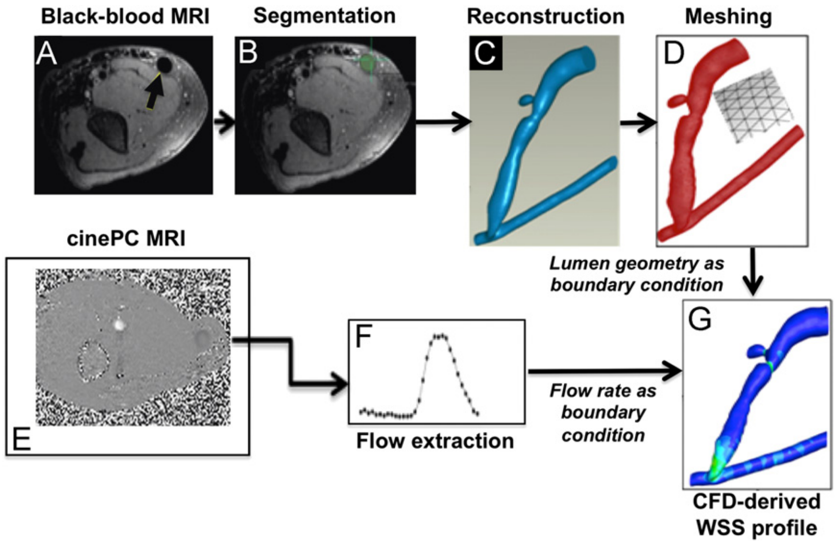

Fig. 1. (Color online) MRI-to-CFD pipeline. The pipeline to obtain the lumen geometry that served as the structural boundary for CFD is shown in Panels A–D. (A) Black-blood (BB) MRI was performed to image lumen geometry. An example DICOM image from the scan shows a cross-section of the arm (arrow indicates fistula vein). (B) Segmentation was performed on the same example DICOM image (fistula vein lumen filled green). (C) The segmented lumen slices were reconstructed and (D) meshed. Panels E–F show the pipeline to obtain blood flow rates used as flow boundary conditions in the CFD. (E) Cine phase-contrast (PC) MRI was performed over a cardiac cycle and (F) blood flow rates during a cardiac cycle were extracted from the cine PC data. Panel G shows a derived wall shear stress (WSS) profile.

Table 1
Contrast-free MR image acquisition protocol.

Scan	Purpose	Imaging parameters
2D BB TSE/FSE with DIR preparation	Obtain images of lumen geometry (lower resolution but less affected by flow artifacts)	TE/TR=8.8/915, echo train length 9, pixel bandwidth 250 Hz, 0.5 mm × 0.5 mm × 2.0 mm (interpolated to 0.25 mm × 0.25 mm × 2.0 mm)
3D BB TSE/FSE with DIR preparation	Obtain images of lumen geometry (higher resolution but more affected by flow artifacts)	TE/TR=24/700, echo train length 39, pixel bandwidth 520 Hz, 0.5 mm × 0.5 mm × 1.0 mm (interpolated to 0.25 mm × 0.25 mm × 1.0 mm)
2D TOF	Identify locations for 2D cine phase-contrast imaging	TE/TR=7/25, pixel bandwidth 80 Hz, 0.3 mm × 0.3 mm × 2.0 mm TE/TR=3.6/25, pixel bandwidth 260 Hz, 0.7 mm × 0.7 mm × 3.0 mm
2D cine phase-contrast	Obtain blood flow rate	TE/TR=3.6/25, pixel bandwidth 260 Hz, 0.7 mm × 0.7 mm × 3.0 mm

Note: BB=black-blood; TSE=turbo-spin echo; FSE=fast-spin echo; DIR=double inversion recovery; TOF=time-of-flight; TE=echo time; TR=repetition time

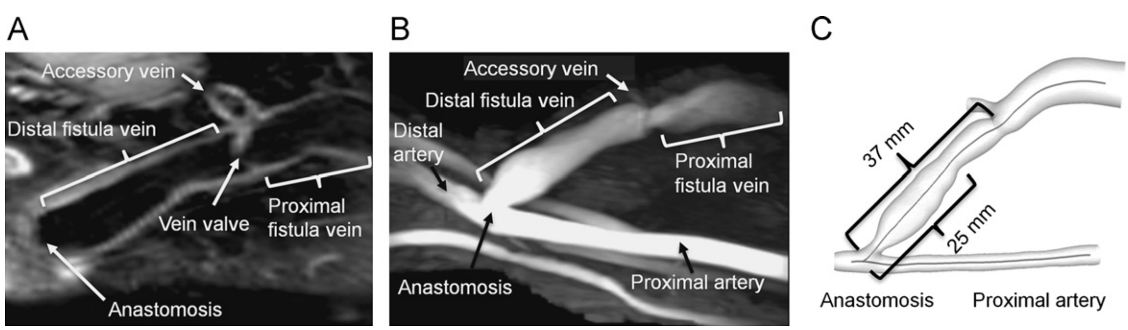

Fig. 2. Configuration and lumen centerlines of the AVF. (A) A multiplanar view of black-blood images of the AVF. The lumen of the fistula vein, the lumen of an accessory vein, and a vein valve (near the accessory vein) are clearly visible. The artery and extraneous vessels are not visible in this view. (B) A maximum-intensity projection of a time-of-flight image of the same AVF. The end-to-side anastomosis of this brachiocephalic AVF is clearly seen. Extraneous vessels are visible running parallel to the brachial artery. The arterial segment upstream to the anastomosis is termed proximal as it is closer to the heart; its blood flow was from the right of the image to the left. The fistula vein is designated as the proximal (closer to the heart) or distal section separated by the accessory vein. (C) The calculated lumen centerlines are shown in the fistula vein and the proximal artery of the 3D reconstruction of the same AVF. The labeled distances correspond to the two troughs shown in Fig. 4A.

and 7 months after AVF creation. The patient was in a supine position with the AVF arm parallel to the body during imaging. Two radio-frequency receive-only phased-array coils were positioned over the AVF. MRI used a Siemens Trio 3T scanner and parameters described in Table 1 (Terry et al., 2009). The total patient preparation and scan time was within one hour.

2.2. Black-Blood (BB) MRI

Lumen images were obtained using two-dimensional (2D) (at 4 months) or 3D BB (5 and 7 months) scans. A BB slice is shown in Fig. 1A. A multiplanar view of the BB scan is shown in Fig. 2A.

2.3. AVF reconstruction and meshing

AVF lumen segmentations and reconstructions (Fig. 1B–C) were performed on the BB images using Amira. Imaging artifacts were removed and all ends were sliced to obtain sharp ends using Geomagic Studio. A high-resolution mesh with approximately 0.9 million cells (Fig. 1D) was generated in Ansys Gambit. Straight extensions were added at all inlets and outlets. Higher-resolution prismatic boundary layers were generated near the wall. Tetrahedral cells were generated in the remaining lumen. The maximal value of equi-size skew of the boundary layers was 0.46, while it was 0.77 for tetrahedral cells. Independence of WSS on mesh density was verified.